ACCEPTED MANUSCRIPT
Journal of Applied Physics
AIP Publishing
This is the author's peer reviewed, accepted manuscript. However, the online version of record will be different from this version once it has been copyedited and typeset.
PLEASE CITE THIS ARTICLE AS DOI: 10.1063/5.0021089

Acceptor complex signatures in oxygen-rich ZnO thin films implanted with chlorine ions

Alexander Azarov[1,a)], Augustinas Galeckas[1], Vishnukanthan Venkatachalapathy[1,2], Zengxia Mei[3,4], Xiaolong Du[3,4], Eduard Monakhov[1], and Andrej Kuznetsov[1]

[1] *University of Oslo, Department of Physics, Centre for Materials Science and Nanotechnology, PO Box 1048 Blindern, N-0316 Oslo, Norway*

[2] *Department of Materials Science, National Research Nuclear University MEPhI, 31 Kashirskoe hwy, 115409 Moscow, Russia*

[3] *Institute of Physics, The Chinese Academy of Sciences, Beijing 100190, China*

[4] *Songshan Lake Materials Laboratory, Dongguan, Guangdong 523808, China*

Spectroscopic identification of defects and impurities is crucial for understanding doping asymmetry issue in ZnO and, therefore, realization of true ZnO-based bipolar devices. Chlorine (Cl) is an amphoteric impurity in ZnO exhibiting acceptor behavior in interstitial configuration (Cl_i) and donor action once on substitutional oxygen sites (Cl_O). In its turn, incorporation of Cl atoms depends on the material growth conditions and a Cl_O fraction should be suppressed in O-rich material. In the present work, Cl ions were implanted into ZnO thin films synthesized under O-rich conditions. In contrast to a negligible effect of Cl incorporation to electrical conductivity, photoluminescence measurements revealed dramatic developments of optical properties with a strong acceptor-like spectral signature emerging after 900°C anneals. We discuss the origins of a new excitonic I* line (3.355 eV) induced by Cl-implantation and propose two alternative defect models based on shallow-acceptor and shallow-donor complexes.

[a)] alexander.azarov@smn.uio.no

ACCEPTED MANUSCRIPT
Journal of Applied Physics
AIP Publishing
This is the author's peer reviewed, accepted manuscript. However, the online version of record will be different from this version once it has been copyedited and typeset.
PLEASE CITE THIS ARTICLE AS DOI: 10.1063/5.0021089

I. Introduction

ZnO is a semiconductor with a wide direct-type bandgap (3.37 eV) as well as large free exciton binding energy (60 meV), which surpass favorably that of GaN (25 meV), the dominating material in the UV-optoelectronics nowadays. However, important unresolved issues in ZnO, related to the insufficient understanding the intrinsic defects, impurities as well as their interaction and evolution, limit the full-scale realization of ZnO potential in optoelectronics [1,2,3,4]. For example, the challenges with *p*-type doping in ZnO are often attributed to the formation of compensation-type defect complexes involving so-called "hole killers", such as Zn interstitials (Zn_i) or oxygen vacancies (V_O), in addition to self-compensation effects and interaction of dopants with residual impurities [5,6].

Among the O-substituting group-VII elements, halogens F and Cl are of particular interest because of their amphoteric behavior, i.e. Cl and F exhibit acceptor behavior in interstitial (Cl_i/F_i) configuration and donor action once positioned on substitutional oxygen sites (Cl_O/F_O) [7-9]. At present, the reports in the literature on the energetics and electronic action of Cl/F dopants are limited and rather contradictory. Despite the fact that F_O demonstrates a relatively high electrical activation and potentially can be used for heavy *n*-type doping of ZnO [10-12]), F atoms exhibit low thermal stability and readily out-diffuse already at moderate temperatures [12,13]. According to the first principles calculations, both Cl_i and Cl_O configurations in ZnO have relatively high ionization energies and thus cannot provide carriers at room temperature (RT) [8]. On the other hand, it has been demonstrated that Cl is an effective donor impurity, and electron concentrations up to 10^{20} cm^{-3} have been reported in Cl-doped ZnO thin films [14,15]. Thus, understanding / control of the dopant incorporation is of paramount importance for the successful realization of ZnO-based devices.

ACCEPTED MANUSCRIPT
Journal of Applied Physics
AIP Publishing
This is the author's peer reviewed, accepted manuscript. However, the online version of record will be different from this version once it has been copyedited and typeset.
PLEASE CITE THIS ARTICLE AS DOI: 10.1063/5.0021089

The material growth conditions play a crucial role on the incorporation of dopants and, therefore, their electronic action. Thus, the transition between O-poor to O-rich condition in ZnO may dramatically affect the defect balance and dopant incorporation [16]; however, this effect is poorly investigated. In the present contribution, we study electrical activation and defect evolution in Cl-implanted ZnO samples synthesized under O-rich conditions, where Cl_O fraction is expected to be suppressed. We demonstrate that even though the implanted Cl ions do not contribute substantially to electrical conductivity at RT, a strong PL signature associated with deep acceptor states emerges upon Cl incorporation and remains stable for the post-annealing temperatures higher than 900 °C.

II. Experimental

Wurtzite ZnO thin films (~550 nm thick) were synthesized at 600° C by radio-frequency plasma-assisted molecular beam epitaxy on *c*-oriented Al_2O_3 substrates. The samples were grown under O-rich conditions and details of the growth can be found elsewhere [17]. The samples were implanted consequently with 300 and 600 keV $^{35}Cl^+$ ions to ion doses of 1×10^{14} and 2×10^{14} cm^{-2}, respectively. The ion energies and doses were chosen in such a way that ensured uniform Cl distribution throughout the ZnO film. The implantations were performed at RT maintaining 7 degrees off-angle orientation from [0001] direction to reduce channeling. The unimplanted and Cl-implanted samples were annealed in air at 500–1000 °C for 30 min using a conventional tube furnace.

The concentration of Cl atoms were measured by secondary ion mass spectrometry (SIMS) using a Cameca IMS 7f microanalyzer with 15 keV Cs^+ ions as primary beam. The intensity-concentration calibration was performed using ion implanted reference ZnO sample. The photoluminescence (PL) measurements were carried out in the

Journal of Applied Physics
ACCEPTED MANUSCRIPT
AIP Publishing
This is the author's peer reviewed, accepted manuscript. However, the online version of record will be different from this version once it has been copyedited and typeset.
PLEASE CITE THIS ARTICLE AS DOI: 10.1063/5.0021089

temperature range 8 - 300 K by employing close-cycle He refrigerator system and using 325 nm wavelength cw He-Cd laser as an excitation source (power density ~20 W/cm^2). The PL spectra were recorded by fiber optic spectrometers (Ocean Optics HR4000/USB4000) with spectral resolution below 0.2 nm / 2 nm, respectively.

III. Results and discussion

The RT electron concentrations and Cl content after anneals are shown in Fig. 1. One can observe that Cl implantation does not lead to any significant increase of the electron concentration for the temperature anneals below 800 °C, whereas comparison of Cl content and carrier concentration suggests that the majority of Cl atoms are electrically inactive at RT. It is worth noting that enhanced electron concentration in the as-implanted sample as compared to unimplanted one is not surprising and it could be attributed to the electrically active radiation defects. Higher temperatures lead to the loss of Cl atoms due to out-diffusion, while the electron concentration starts to increase in both Cl-implanted and unimplanted samples, which is likely related to thermal activation of residual impurities and in-diffusion of Al atoms from the substrate.

Fig. 2 summarizes PL results obtained at 10K of as-grown, as-implanted and post-annealed samples. The as-grown sample exhibits spectral features characteristic to high crystal quality ZnO with an intense near-band-edge (NBE) component dominating over a broad deep-level emission (DLE) band. One can observe in Fig. 2(a) that defect-related DLE comprises multiple overlapping bands with two major emissions in the green and red regions of spectra. It is worth noting at this point that the assignments of optical transitions to DLE peaks are often contradictory in the literature and remain a subject of debate. The so-called red luminescence (RL) in the 1.6-1.8 eV region is commonly associated with open volume defects such as zinc vacancy (V_{Zn}) clusters [18,4], and/or with oxygen interstitials O_i [21]. The origin of the green luminescence

ACCEPTED MANUSCRIPT
Journal of Applied Physics
AIP Publishing
This is the author's peer reviewed, accepted manuscript. However, the online version of record will be different from this version once it has been copyedited and typeset.
PLEASE CITE THIS ARTICLE AS DOI: 10.1063/5.0021089

(GL) within the range 2.3-2.5 eV remains controversial with several emission mechanisms proposed that involve V_O [19, 20] and oxygen interstitials (O_i) [22], V_{Zn} [23, 24] and V_{Zn}-donor complexes [25], Zn_i [26] and antisites (O_{Zn}) [27], copper impurities [28, 29], and surface states [30]. In theory, the most likely candidate for GL is isolated V_{Zn} offering a deep acceptor state with a low formation energy according to the first-principles calculations [31]. It should be noted that while theoretical predictions assume defect formation under thermodynamic equilibrium conditions, ZnO material in the present study was grown under O-rich conditions that make V_O less favorable candidate for GL among other alternatives.

The as-implanted sample exhibits very low total luminescence yield, which is indicative of multiple non-radiative recombination pathways introduced by ion implantation damage. Within DLE range, a distinctive broad RL band (at 1.8 eV with FWHM of 0.5 eV) is the only spectral feature. The post-implantation annealings performed to alleviate the crystal damage also markedly enhanced RL already after 500 °C, and GL after 700 °C anneals. Further annealings at higher temperatures increase both RL and GL bands, albeit at different pace, as shown in the Inset in Fig. 2(a). The initial dominance of RL implies the prevalence of V_{Zn} clusters and/or O_i's in as-implanted material. As the annealing temperature is increased, GL is rising, while RL signal saturates indicating the intrinsic defects balance change in favor of isolated V_{Zn} and/or V_O luminescent centers. Other than that, there are no apparent new features emerging in the DLE region that could be uniquely attributed to the incorporated Cl ions. However, such Cl-implantation induced developments clearly take place in the excitonic region of the spectra.

The thermal evolutions of the NBE peaks in unimplanted and Cl-implanted samples are plotted alongside for comparison in Figs. 2(b, c). Here, a set of vertical drop lines marks the energy positions and labeling of the excitonic emission lines established in

ACCEPTED MANUSCRIPT
Journal of Applied Physics
AIP Publishing
This is the author's peer reviewed, accepted manuscript. However, the online version of record will be different from this version once it has been copyedited and typeset.
PLEASE CITE THIS ARTICLE AS DOI: 10.1063/5.0021089

the literature [32, 33]. In addition, a reference spectrum obtained from a high-crystallinity bulk ZnO is presented in Fig. 2(b), where the free-exciton transition involving A-valence band (FX_A) can be observed at 3.375 eV providing a benchmark for estimation of exciton localization energies.

The as-grown ZnO (unimplanted sample prior to annealing) demonstrates strong NBE peak at around 3.36 eV with an extensive high-energy shoulder originating from several donor bound exciton (DX) transitions labeled as I2 through I8 in Fig. 2. The annealing leads to apparent narrowing of the NBE emission as the I2-I4 transitions are suppressed and only I6-I8 contributions prevail. By contrast, Cl-implanted ZnO shows dominance of the I5-I8 lines for the temperatures up to 900 °C, whereupon a new emission line emerges at 3.355 eV (labeled I* in Fig. 2(c)) and becomes the most prominent NBE feature after annealing at 1000°C. It should be noted that only a few I-lines are unambiguously linked to chemical elements such as H, Al, Ga and In [33], thus leaving a possibility that the incorporated Cl is behind some of those yet unidentified. Indeed, chlorine was identified as a shallow donor in the early electron paramagnetic resonance work of Kasai [34], and there is indirect evidence that I5 might be caused by Cl [35].

The suppressed shoulder upon annealing of unimplanted ZnO is indicative of hydrogen (I4) loss (diffusion, complexing, etc.) during thermal treatment. Thermally resilient I6/I8 lines are common and often-dominating NBE features (c.f. spectrum of bulk ZnO in Fig. 2(b)) associated with Al and Ga impurities, respectively [33]. The new emission line I* (3.355 eV) emerges in between I9 (3.357eV) and I10 (3.353eV) lines, which are associated to neutral donor-bound excitons (D^0X) involving In and Sn, respectively [33, 36]. To our knowledge, there is no defect assignment for this I* line position in the literature. It should be noted that I9-I11 spectral region has long been considered for possible manifestation of neutral acceptor-bound excitons (A^0X) [37],

Journal of Applied Physics
ACCEPTED MANUSCRIPT
AIP Publishing
This is the author's peer reviewed, accepted manuscript. However, the online version of record will be different from this version once it has been copyedited and typeset.
PLEASE CITE THIS ARTICLE AS DOI: 10.1063/5.0021089

though presently such association is disputed [35]. The distinction between donor and acceptor bound excitons is complicated by the fact that their localization energies (E_{loc}) overlap in the range from 16 to 25 meV [38]. As for the excitonic I* emission, the localization energy of E_{loc} = 20 meV is determined from the energy separation between this line (3.355 eV) and the free transversal A exciton (A_T = 3.375eV) in Fig. 2(c). Next, the energy position of the respective donor or acceptor states then can be approximated for the given localization energy by applying Haynes rule [39]. Assuming D^0X origin of I* line, the donor binding energy (E_D) can be estimated from the Haynes relationship $E_{loc} = 0.365\times E_D - 3.8$ meV [33] with the resultant E_D = 65.2 meV. A representative feature of donor-bound excitons is the two-electron satellite (TES) transitions [33], however, the expected signature at around 3.306 eV is not noticeable in the PL spectra. As mentioned earlier, a neutral acceptor-bound exciton (A^0X) origin has also been considered for the lines observed in this spectral region [33, 40, 41]. By employing Haynes rule for acceptors [38], the estimated acceptor binding energy E_A would be in the range 140-210 meV.

The identification of specific exciton lines also requires differentiating excitons in the excited state from those in the ground state, which can be recognized from different thermal evolution of the related emission lines. Temperature-dependent PL measurements (8 to 200 K) were performed to verify whether Cl-implantation induced recombination line I* (3.355 eV) involves ground or excited excitonic states. For comparison, the intensities of I* and I8 recombination lines versus temperature are shown in the Arrhenius plot in Fig. 3. The peak intensities of both I* and I8 decrease monotonically with increasing temperature, which is typical behavior of donor-bound excitons in their ground state [35, 42]. The solid lines in Fig. 3 represent fits to the data from which the activation energies were obtained following the procedure described in [43]. The activation energies of 17.6 and 19.7 meV derived for the ground state

Journal of Applied Physics
ACCEPTED MANUSCRIPT
AIP Publishing
This is the author's peer reviewed, accepted manuscript. However, the online version of record will be different from this version once it has been copyedited and typeset.
PLEASE CITE THIS ARTICLE AS DOI: 10.1063/5.0021089

emission lines I8 and I* are consistent with the corresponding localization energies (16 and 20 meV) estimated from spectra in Fig. 2(c). At elevated temperatures approaching 200 K, both emission lines are thermally quenched with similar activation energy of ~57 meV, which agrees well with the free-exciton binding energy.

Below we discuss possible scenarios of Cl incorporation into ZnO taking into account the reported theoretical predictions [8]. Despite that the first-principles pseudopotential calculations on the Cl-doped ZnO suggest that the substitutional Cl_O is energetically more favorable to form during the growth as compared to interstitial Cl_i sites, both Cl_i and C_O sites can be generated in Cl-implanted ZnO. Theory predicts very deep states for both acceptor-like Cl_i (E_V+0.806 eV) and donor-like Cl_O (E_C-0.553 eV) implying that neither can contribute to electrical properties at RT, as indeed is evidenced in this study. However, presumably Cl-related excitonic features in the NBE region of PL spectra (I5 and I* lines) cannot be directly linked to such deep donor and acceptor states as predicted by theory. Indeed, the localization energy of I* line (20 meV) indicates that the exciton is bound to either a shallow donor (65.2 meV) or to shallow acceptor (140-210 meV). If the theoretical calculations [8] are correct and the interstitial Cl_i indeed forms a deep acceptor level (E_V+0.8 eV), then the assumed (A^0X) origin of I* line would imply involvement of some form of acceptor-like Cl complex. Such a defect model seems reasonable from the analogy with nitrogen-doped ZnO, where a variety of complexes involving N dopant (V_{Zn}-N_O, $(NH_4)_{Zn}$ and $(N_2)_{Zn}$) are considered for the role of shallow acceptors [44]. The fact that ZnO in the present study was grown under oxygen-rich conditions ensures the abundance of zinc vacancies. Furthermore, as it has been mentioned above, Cl_O can be generated in Cl-implanted ZnO, therefore, formation of stable (V_{Zn}-Cl_O) complexes promoted by Coulomb interaction cannot be excluded. High probability of formation of such acceptorlike compensation complexes was also supported by a thermodynamic analysis [45].

Journal of Applied Physics
ACCEPTED MANUSCRIPT
AIP Publishing
This is the author's peer reviewed, accepted manuscript. However, the online version of record will be different from this version once it has been copyedited and typeset.
PLEASE CITE THIS ARTICLE AS DOI: 10.1063/5.0021089

Apparently, the incorporated chlorine acts as a stabilizing agent for shallow acceptor complexes to survive up to 1000°C annealings. This kind of defect stabilizing effect has been observed earlier for nitrogen dopants in ZnO [46,47].

The alternative model of shallow-donor related origin of I* considers pairing of donors and acceptors as a neutral complex to which excitons can bind. The existence of such shallow donor complex (Zn_i-N_O) has been proven in nitrogen-doped ZnO [48]; reportedly, also other combinations of Zn interstitial-acceptor pairs that produce bound states may exist - hence, we assume that such a paired acceptor could be the interstitial Cl_i.

IV. Conclusions

In summary, Cl ions were implanted into ZnO thin films synthesized under O-rich conditions. The implanted Cl atoms remain stable up to 800 °C, above which Cl losses start to increase with the temperature. In contrast to a negligible effect of Cl incorporation on electrical conductivity, PL measurements show dramatic developments of optical properties with a strong acceptor-like spectral signatures emerging after 900 °C anneals. PL results clearly indicate bound exciton properties, however a decisive identification of the defect causing I* line was not possible. In view of that, two alternative models are proposed that associate I* origin with shallow-acceptor and shallow-donor complexes.

Journal of Applied Physics
AIP Publishing
ACCEPTED MANUSCRIPT
This is the author's peer reviewed, accepted manuscript. However, the online version of record will be different from this version once it has been copyedited and typeset.
PLEASE CITE THIS ARTICLE AS DOI: 10.1063/5.0021089

ACKNOWLEDGMENTS

This work was performed within the Research Centre for Sustainable Solar Cell Technology (FME SuSolTech, project number 257639) and co-sponsored by the Research Council of Norway and industry partners; the partial support from the INTPART project (No 261574) and National Natural Science Foundation of China (No. 11674405) is also kindly acknowledged.

DATA AVAILABILITY

The data that supports the findings of this study are available within the article.

ACCEPTED MANUSCRIPT
Journal of Applied Physics
AIP Publishing
This is the author's peer reviewed, accepted manuscript. However, the online version of record will be different from this version once it has been copyedited and typeset.
PLEASE CITE THIS ARTICLE AS DOI: 10.1063/5.0021089

References

1. A. B. Djurišić, A. M. C. Ng, and X. Y. Chen, "ZnO nanostructures for optoelectronics: Material properties and device applications", Prog. in Quantum Electronics **34,** 191 (2010). https://doi.org/10.1016/j.pquantelec.2010.04.001
2. Ü. Özgür, Y. I. Alivov, C. Liu, A. Teke, M. A. Reshchikov, S. Doğan, V. Avrutin, S.-J. Cho, and H. Morkoç, "A comprehensive review of ZnO materials and devices", J. Appl. Phys. **98,** 041301 (2005). https://doi.org/10.1063/1.1992666
3. J. Lv, C. Li, and Z. Chai, "Defect luminescence and its mediated physical properties in ZnO", J. Luminescence **208,** 225 (2019). https://doi.org/10.1016/j.jlumin.2018.12.050
4. K. E. Knutsen, A. Galeckas, A. Zubiaga, F. Tuomisto, G. C. Farlow, B. G. Svensson, and A. Yu. Kuznetsov, "Zinc vacancy and oxygen interstitial in ZnO revealed by sequential annealing and electron irradiation", Phys. Rev. B **86,** 121203(R) (2012). https://doi.org/10.1103/PhysRevB.86.121203
5. C. H. Park, S.B. Zhang, and S.-H. Wei, "Origin of *p*-type doping difficulty in ZnO: The impurity perspective", Phys. Rev. B **66,** 073202 (2002). https://doi.org/10.1103/PhysRevB.66.073202
6. V. Avrutin, D. J. Silversmith, and H. Morkoç, "Doping asymmetry problem in ZnO: Current status and outlook", Proceedings of the IEEE **98,** 1269 (2010). https://doi.org/10.1109/JPROC.2010.2043330
7. A. Janotti**,** E. Snow, and C. G. Van de Walle, "A pathway to *p*-type wide-band-gap semiconductors", Appl. Phys. Lett. **95,** 172109 (2009). https://doi.org/10.1063/1.3247890
8. B. Liu, M. Gu, X. Liu, S. Huang, and C. Ni, "Defect formation in chlorine-doped zinc oxide", Solid State Communications **171,** 30 (2013). https://doi.org/10.1016/j.ssc.2013.06.026

Journal of Applied Physics
ACCEPTED MANUSCRIPT
AIP Publishing
This is the author's peer reviewed, accepted manuscript. However, the online version of record will be different from this version once it has been copyedited and typeset.
PLEASE CITE THIS ARTICLE AS DOI: 10.1063/5.0021089

9. B. Liu, M. Gu, X. Liu, S. Huang, and C. Ni, “First-principles study of fluorine-doped zinc oxide”, Appl. Phys. Lett. **97,** 122101 (2010). https://doi.org/10.1063/1.3492444

10. S. S. Shinde, P. S. Shinde, S. M. Pawar, A. V. Moholkar, C. H. Bhosale, and K. Y. Rajpure, “Physical properties of transparent and conducting sprayed fluorine doped zinc oxide thin films”, Solid State Sciences **10,** 1209 (2008). https://doi.org/10.1016/j.solidstatesciences.2007.11.031

11. H. Y. Xu, Y. C. Liu, R. Mu, C. L. Shao, Y. M. Lu, D. Z. Shen, and X. W. Fan, “F-doping effects on electrical and optical properties of ZnO nanocrystalline films”, Appl. Phys. Lett. **86,** 123107 (2005). https://doi.org/10.1063/1.1884256

12. A. Azarov, V. Venkatachalapathy, Z. Mei, L. Liu, X. Du, A. Galeckas, E. Monakhov, B. G. Svensson, and A. Kuznetsov, “Self-diffusion measurements in isotopic heterostructures of undoped and *in situ* doped ZnO: Zinc vacancy energetics”, Phys. Rev. B **94,** 195208 (2016). https://doi.org/10.1103/PhysRevB.94.195208

13. A. Yu. Azarov, B. G. Svensson, and A. Yu. Kuznetsov, “Impurity-limited lattice disorder recovery in ion-implanted ZnO”, Appl. Phys. Lett. **101,** 222109 (2012). https://doi.org/10.1063/1.4768289

14. E. Chikoidze, M. Nolan, M. Modreanu, V. Sallet, and P. Galtier, “Effect of chlorine doping on electrical and optical properties of ZnO thin films”, Thin Solid Films **516,** 8146 (2008). https://doi.org/10.1016/j.tsf.2008.04.076

15. F. Wang, J.-H. Seo, Z. Li, A. V. Kvit, Z. Ma, and X. Wang, “Cl-doped ZnO nanowires with metallic conductivity and their application for high-performance photoelectrochemical electrodes”, ACS Appl. Mater. Interfaces **6,** 1288 (2014). https://doi.org/10.1021/am405141s

16. V. Venkatachalapathy, A. Galeckas, A. Zubiaga, F. Tuomisto, and A. Yu. Kuznetsov, “Changing vacancy balance in ZnO by tuning synthesis between

ACCEPTED MANUSCRIPT
Journal of Applied Physics
AIP Publishing
This is the author's peer reviewed, accepted manuscript. However, the online version of record will be different from this version once it has been copyedited and typeset.
PLEASE CITE THIS ARTICLE AS DOI: 10.1063/5.0021089

zinc/oxygen lean conditions", J. Appl. Phys. **108**, 046101 (2010). https://doi.org/10.1063/1.3462394

17. L. Liu, Z. Mei, A. Tang, A. Azarov, A. Kuznetsov, Q.-K. Xue, and X. Du, "Oxygen vacancies: The origin of *n*-type conductivity in ZnO", Phys. Rev. B **93**, 235305 (2016). https://doi.org/10.1103/PhysRevB.93.235305

18. Y. Dong, F. Tuomisto, B. G. Svensson, A. Yu. Kuznetsov, and L. J. Brillson, "Vacancy defect and defect cluster energetics in ion-implanted ZnO", Phys. Rev. B **81,** 081201(R) (2010). https://doi.org/10.1103/PhysRevB.81.081201

19. K. Vanheusden, C. H. Seager, W. L. Warren, D. R. Tallant, and J. A. Voigt, "Correlation between photoluminescence and oxygen vacancies in ZnO phosphors", Appl. Phys. Lett. **68,** 403 (1996). https://doi.org/10.1063/1.116699

20. F. Leiter, H. Alves, D. Pfisterer, **N.** G. Romanov, D. M. Hofmann, and B. K. Meyer, "Oxygen vacancies in ZnO", Physica B **340,** 201 (2003). https://doi.org/10.1016/j.physb.2003.09.031

21. C. H. Ahn, Y. Y. Kim, D. C. Kim, S. K. Mohanta, and H. K. Cho, "A comparative analysis of deep level emission in ZnO layers deposited by various methods", J. Appl. Phys. **105,** 013502 (2009). https://doi.org/10.1063/1.3054175

22. M. Liu, A.H. Kitai, and P. Mascher, "Point defects and luminescence centres in ZnO and Mn-doped ZnO", J. Luminescence **54,** 35 (1992). https://doi.org/10.1016/0022-2313(92)90047-D

23. T. M. Børseth, B. G. Svensson, A. Yu. Kuznetsov, P. Klason, Q. X. Zhao, and M. Willander, "Identification of oxygen and zinc vacancy optical signals in ZnO", Appl. Phys. Lett. **89,** 262112 (2006). https://doi.org/10.1063/1.2424641

24. A. Janotti and C. G. V. de Walle, "Fundamentals of zinc oxide as a semiconductor", Rep. Prog. Phys. **72,** 126501 (2009). https://doi.org/10.1088/0034-4885/72/12/126501

Journal of Applied Physics
ACCEPTED MANUSCRIPT
AIP Publishing
This is the author's peer reviewed, accepted manuscript. However, the online version of record will be different from this version once it has been copyedited and typeset.
PLEASE CITE THIS ARTICLE AS DOI: 10.1063/5.0021089

25. Y. K. Frodason, K. M. Johansen, T. S. Bjørheim, B. G. Svensson, and A. Alkauskas, "Zn vacancy-donor impurity complexes in ZnO", Phys. Rev. B **97,** 104109 (2018). https://doi.org/10.1103/PhysRevB.97.104109

26. N. O. Korsunska, L. V. Borkovska, B. M. Bulakh, L. Y. Khomenkova, V. I. Kushnirenko, and I. V. Markevich, "The influence of defect drift in external electric field on green luminescence of ZnO single crystals", J. Luminescence **102,** 733 (2003). https://doi.org/10.1016/S0022-2313(02)00634-8

27. B. Lin, Z. Fu, and Y. Jia, "Green luminescent center in undoped zinc oxide films deposited on silicon substrates", Appl. Phys. Lett. **79,** 943 (2001). https://doi.org/10.1063/1.1394173

28. N. Y. Garces, L. Wang, L. Bai, N. C. Giles, L. E. Halliburton, and G. Cantwell, "Role of copper in the green luminescence from ZnO crystals", Appl. Phys. Lett. **81,** 622 (2002). https://doi.org/10.1063/1.1494125

29. R. Dingle, "Luminescent transitions associated with divalent copper impurities and the green emission from semiconducting Zinc Oxide", Phys. Rev. Lett. **23,** 579 (1969). https://doi.org/10.1103/PhysRevLett.23.579

30. S. Monticone, R. Tufeu, and A. V. Kanaev, "Complex nature of the UV and visible fluorescence of colloidal ZnO nanoparticles", J. Phys. Chem. B **102,** 2854 (1998). https://doi.org/10.1021/jp973425p

31. A. Janotti and C. G. Van de Walle, "Native point defects in ZnO", Phys. Rev. B **76,** 165202 (2007). https://doi.org/10.1103/PhysRevB.76.165202

32. D. C. Reynolds, C. W. Litton, and T. C. Collins, "Zeeman effects in the edge emission and absorption of ZnO", Phys. Rev. **140,** A1726 (1965). https://doi.org/10.1103/PhysRev.140.A1726

33. B. K. Meyer, H. Alves, D. M. Hofmann, W. Kriegseis, D. Forster, F. Bertram, J. Christen, A. Hoffmann, M. Straßburg, M. Dworzak, U. Haboeck, and A. V.

ACCEPTED MANUSCRIPT
Journal of Applied Physics
AIP Publishing
This is the author's peer reviewed, accepted manuscript. However, the online version of record will be different from this version once it has been copyedited and typeset.
PLEASE CITE THIS ARTICLE AS DOI: 10.1063/5.0021089

Rodina, "Bound exciton and donor–acceptor pair recombinations in ZnO", Phys. Status Solidi B **241,** 231 (2004). https://doi.org/10.1002/pssb.200301962

34. P. H. Kasai, "Electron spin resonance studies of donors and acceptors in ZnO", Phys. Rev. **130,** 989 (1963). https://doi.org/10.1103/PhysRev.130.989

35. B. K. Meyer, J. Sann, S. Eisermann, S. Lautenschlaeger, M. R. Wagner, M. Kaiser, G. Callsen, J. S. Reparaz, and A. Hoffmann, "Excited state properties of donor bound excitons in ZnO", Phys. Rev. B **82,** 115207 (2010). https://doi.org/10.1103/PhysRevB.82.115207

36. J. Cullen, D. Byrne, K. Johnston, E. McGlynn, and M. O. Henry, "Chemical identification of luminescence due to Sn and Sb in ZnO", Appl. Phys. Lett. **102,** 192110 (2013). https://doi.org/10.1063/1.4807288

37. J. Gutowski, N. Presser, and I. Broser, "Acceptor-exciton complexes in ZnO: A comprehensive analysis of their electronic states by high-resolution magnetooptics and excitation spectroscopy", Phys. Rev. B **38,** 9746 (1988). https://doi.org/10.1103/PhysRevB.38.9746

38. B. K. Meyer, J. Sann, S. Lautenschlaeger, M. R. Wagner, and A. Hoffmann, "Ionized and neutral donor-bound excitons in ZnO", Phys. Rev. B **76,** 184120 (2007). https://doi.org/10.1103/PhysRevB.76.184120

39. J. R. Haynes, "Experimental proof of the existence of a new electronic complex in Silicon", Phys. Rev. Lett. **4,** 361 (1960). https://doi.org/10.1103/PhysRevLett.4.361

40. B. Meyer, J. Stehr, A. Hofstaetter, N. Volbers, A. Zeuner, and J. Sann, "On the role of group I elements in ZnO", Appl. Phys. A **88,** 119 (2007). https://doi.org/10.1007/s00339-007-3962-4

41. K. Tang, R. Gu, S. Zhu, Z. Xu, Y. Shen, J. Ye, and S. Gu, "Optical fingerprints of donors and acceptors in high-quality NH_3-doped ZnO films", Opt. Mater. Express **7,** 1169 (2017). https://doi.org/10.1364/OME.7.001169

ACCEPTED MANUSCRIPT
Journal of Applied Physics
AIP Publishing
This is the author's peer reviewed, accepted manuscript. However, the online version of record will be different from this version once it has been copyedited and typeset.
PLEASE CITE THIS ARTICLE AS DOI: 10.1063/5.0021089

42. R. J. Mendelsberg, M. W. Allen, S. M. Durbin, and R. J. Reeves, "Photoluminescence and the exciton-phonon coupling in hydrothermally grown ZnO", Phys. Rev. B **83,** 205202 (2011). https://doi.org/10.1103/PhysRevB.83.205202

43. H. Shibata, "Negative thermal quenching curves in photoluminescence of solids", Jpn. J. Appl. Phys. **37,** 550 (1998). https://doi.org/10.1143/JJAP.37.550

44. K. Tang, S. Zhu, Z. Xu, J. Ye, and S. Gu, "Experimental investigation on nitrogen related complex acceptors in nitrogen-doped ZnO films", Journal of Alloys and Compounds **696,** 590 (2017). https://doi.org/10.1016/j.jallcom.2016.11.262

45. T. Tchelidze, E. Chikoidze, O. Gorochov, and P. Galtier, "Perspectives of chlorine doping of ZnO", Thin Solid Films **515**, 8744 (2007). https://doi.org/10.1016/j.tsf.2007.04.003

46. A. Azarov, E. Wendler, E. Monakhov, and B. G. Svensson, "Defect stabilization and reverse annealing in ZnO implanted with nitrogen at room and cryogenic temperature", J. Appl. Phys. **123,** 105701 (2018). https://doi.org/10.1063/1.5022152

47. F. Tuomisto, C. Rauch, M. R. Wagner, A. Hoffmann, S. Eisermann, B. K. Meyer, L. Kilanski, M. C. Tarun, and M. D. McCluskey, "Nitrogen and vacancy clusters in ZnO", J. Mater. Res. **28,** 1977 (2013). https://doi.org/10.1557/jmr.2013.195

48. D. C. Look, G. C. Farlow, P. Reunchan, S. Limpijumnong, S. B. Zhang, and K. Nordlund, "Evidence for native-defect donors in n-type ZnO", Phys. Rev. Lett. **95,** 225502 (2005). https://doi.org/10.1103/PhysRevLett.95.225502

Journal of Applied Physics
ACCEPTED MANUSCRIPT
AIP Publishing
This is the author's peer reviewed, accepted manuscript. However, the online version of record will be different from this version once it has been copyedited and typeset.
PLEASE CITE THIS ARTICLE AS DOI: 10.1063/5.0021089

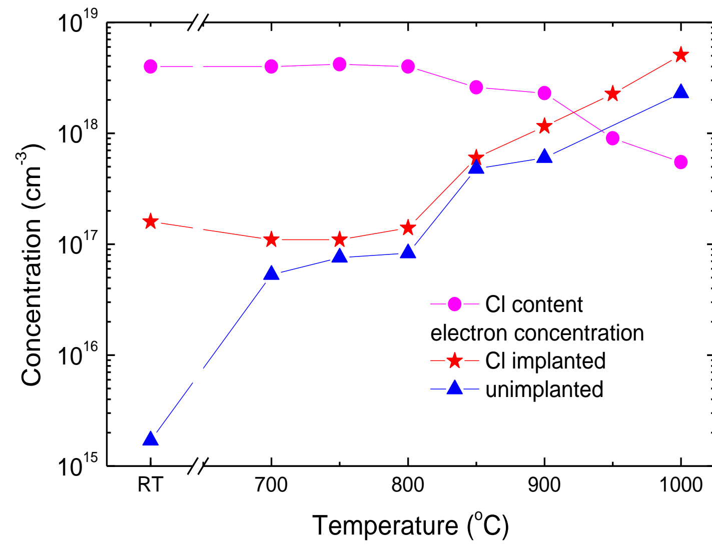

FIG. 1. The retained Cl content and electron concentrations at RT in unimplanted and Cl-implanted ZnO thin films as a function of annealing temperature.

Journal of Applied Physics

ACCEPTED MANUSCRIPT

AIP Publishing

This is the author's peer reviewed, accepted manuscript. However, the online version of record will be different from this version once it has been copyedited and typeset.
PLEASE CITE THIS ARTICLE AS DOI: 10.1063/5.0021089

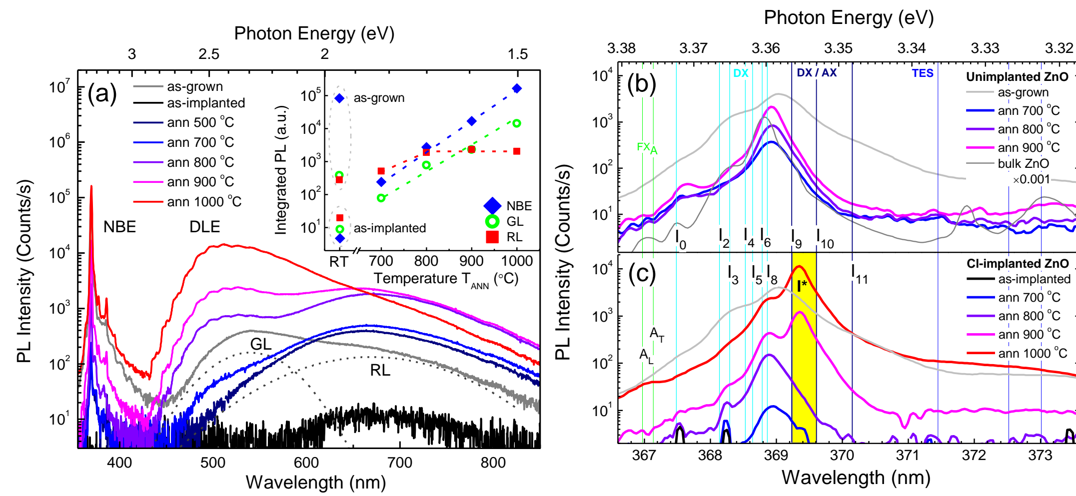

FIG. 2. PL spectra obtained at 10 K of the sample implanted with Cl ions before and after different anneals as indicated in the legend (a). The labels mark key spectral constituents discussed in the text; Gaussian (dashed) curves highlight the RL and GL bands within the multi-component structure of DLE. Inset shows evolution of the integrated PL intensities of the key components as a function of annealing temperature The enlarged NBE region of the unimplanted and implanted samples is shown in the panels (b) and (c), respectively.

ACCEPTED MANUSCRIPT
Journal of Applied Physics
AIP Publishing
This is the author's peer reviewed, accepted manuscript. However, the online version of record will be different from this version once it has been copyedited and typeset.
PLEASE CITE THIS ARTICLE AS DOI: 10.1063/5.0021089

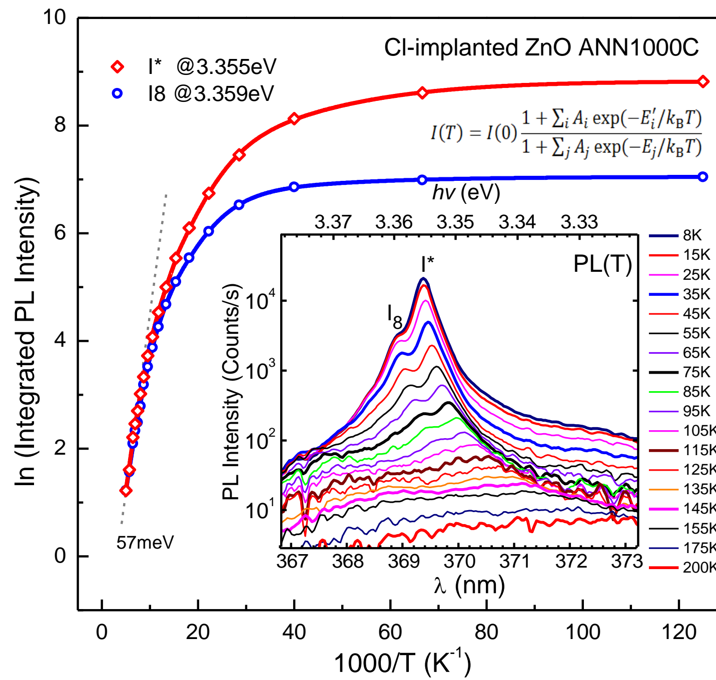

FIG. 3. Arrhenius plot of the integrated PL intensity of I* and I8 lines obtained for Cl-implanted ZnO thin films annealed at 1000°C. Dots are experimental data, and solid lines are numerical fits. Inset depicts evolution of NBE emission with temperature.

AIP Publishing

Journal of Applied Physics

ACCEPTED MANUSCRIPT

This is the author's peer reviewed, accepted manuscript. However, the online version of record will be different from this version once it has been copyedited and typeset.

PLEASE CITE THIS ARTICLE AS DOI: 10.1063/5.0021089

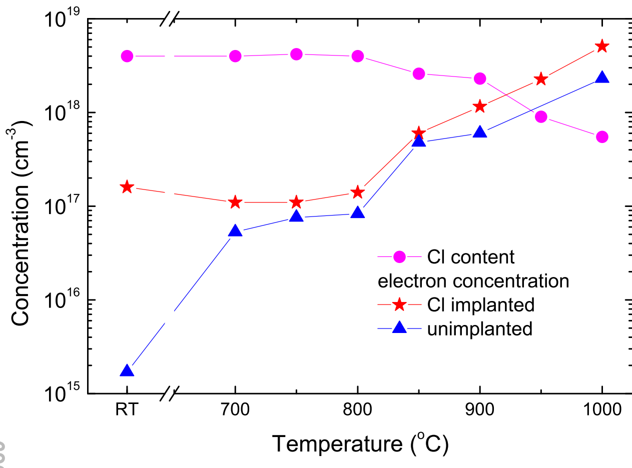

Journal of Applied Physics
ACCEPTED MANUSCRIPT
AIP Publishing
This is the author's peer reviewed, accepted manuscript. However, the online version of record will be different from this version once it has been copyedited and typeset.
PLEASE CITE THIS ARTICLE AS DOI: 10.1063/5.0021089

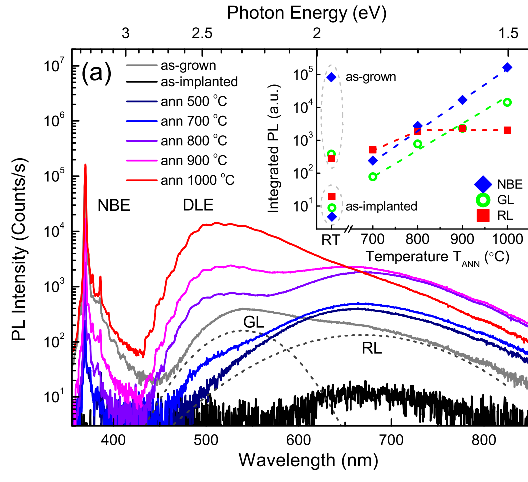

Journal of Applied Physics

ACCEPTED MANUSCRIPT

AIP Publishing

This is the author's peer reviewed, accepted manuscript. However, the online version of record will be different from this version once it has been copyedited and typeset.

PLEASE CITE THIS ARTICLE AS DOI: 10.1063/5.0021089

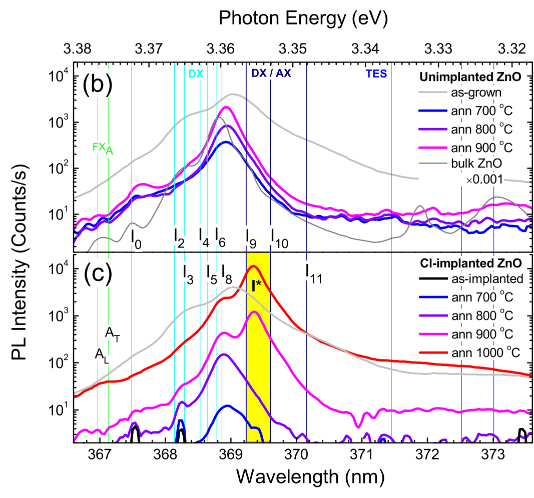

ACCEPTED MANUSCRIPT
Journal of Applied Physics
AIP Publishing
This is the author's peer reviewed, accepted manuscript. However, the online version of record will be different from this version once it has been copyedited and typeset.
PLEASE CITE THIS ARTICLE AS DOI: 10.1063/5.0021089